Shape Analysis of Elastic Curves in Euclidean Spaces

Rayane Mouhli
rayane.mouhli@ensae.fr
MVA – ENS Paris-Saclay
France, Paris

Gabriel Watkinson
gabriel.watkinson@ensae.fr
MVA – ENS Paris-Saclay
France, Paris

1 INTRODUCTION

Shape analysis is a fundamental problem in many fields, including computer vision, medical image analysis, and mechanical engineering. In particular, the analysis of curves and surfaces is an important topic, as it allows the comparison and analysis of shapes of objects in various contexts. For example, a shape metric can quantify the difference between two given shapes regardless of rotation or parametrization. It can also help for registration, which is a method that consists in finding the optimal transformation from one shape to another.

In this paper *Shape Analysis of Elastic Curves in Euclidean Spaces* written by A. Srivastava, E. Klassen, S.H. Joshi I.H. Jermyn, the authors propose a new method for elastic curve analysis that combines a new representation of curves named, the *"square-root velocity"* (SRV) representation with a numerical approach called *"path-straightening"* to find geodesics between shapes of open and closed curves in $\mathbb{R}^n$. The SRV representation is a representation of a curve that captures both its geometry and topology. The *path-straightening* approach uses a gradient-based iteration to find a geodesic between two shapes, and the gradient is available in an analytical form using the Palais metric on the space of paths. The authors also present a gradient-based solution for optimal reparameterization of curves when finding geodesics between their shapes.

2 CONTEXT OF THE PROBLEM

2.1 Previous work

Shape analysis has been extensively studied since the 80s as it is a fundamental problem across many fields. Therefore, many frameworks have been proposed, each with their pros and cons. However, a constant between all the publications is that a shape is defined as the geometry of an object, modulo its position, orientation, and size. This allows to compare objects without having to be too careful about scaling, position, rotation and parametrization. In this framework, two objects are considered identical if they have the same shapes. On another hand, there are many possible representations for a geometrical object, for example :

- **Landmarks :** The idea is that a shape can be represented as a set of identifiable key points. A famous example is a problem asked by David Kendall in 1974 : *"Assuming that I draw 52 points at random in a square, how many flat triangles am I going to observe ?"* This problem led to the publication of many founding articles as *The diffusion of shape*, Kendall (1977) [2] or *Alignments in two-dimensional random sets of points*, Kendall (1980) [3].
- **Boundary models (points, curves, surfaces, level sets) :** This representation is in the same spirit as Kendall's formulation, but it has the advantage to get rid of the landmarks.

Indeed, the use of landmarks can be limiting since the choice of key points are often subjective. Moreover, it is more natural to represent smooth objects with continuous boundaries. This representation is the one we are going to study in this paper.
- **Interior models (medial, solid mesh) :** For instance, the medial axis is the set of all points having more than one closest point on the object's boundary. Then, since the medial axis is "in the middle" of the original shape, it can be assimilated to a skeleton.

A more formal definition of a shape is a point in a high-dimensional manifold called a shape space. First, Laurent Younes in his paper *Computable elastic distances between shapes* [9] defined shape spaces of planar curves and Riemannian metrics on them. As in our paper, closed and open curves are treated differently in order to perform pertinent comparisons while computing geodesic paths for example. This framework led to the publication of many papers on the definition of several Riemannian metrics on spaces of planar curves. Mio et al. [4] presented a family of elastic metrics for functions $\beta : D \to \mathbb{R}^2$. The velocity vector can be written with a speed and an angle term as in our paper : $\dot{\beta}(t) = e^{\phi(t)}e^{i\theta(t)}$ using the identification between $\mathbb{R}^2$ and $\mathbb{C}$. We define the Riemannian metric for $a, b > 0$:

$$\langle (h_1, f_1), (h_2, f_2) \rangle_{(\phi_0, \theta_0)} = a \int_0^1 h_1(t)h_2(t)e^{\phi_0(t)}\mathrm{d}t$$
$$+ b \int_0^1 f_1(t)f_2(t)e^{\phi_0(t)}\mathrm{d}t$$

with (h_1, f_1) and (h_2, f_2) two tangents vectors to $\mathcal{H}$ (the space of all pairs (ϕ, θ)) at (ϕ_0, θ_0).

This is a weighted sum of the standard $\mathbb{L}^2$ inner product with respect to the arc-length element $\mathrm{d}s = e^{\phi(t)}$. The constants a and b can be interpreted as tension and rigidity coefficients. Large values of the ratio $\chi = a/b$ indicate that the material offers higher resistance to stretching and compression than to bending. The opposite holds for χ smalls.

In the case $a = 1$ and $b = 1$, this metric is similar to the one used by Younes in the paper cited above.

Our paper is strongly related to the article presented above, but it extends the method to curves in $\mathbb{R}^n$.

2.2 Target applications

This paper presents a general framework to study shapes in $\mathbb{R}^n$, so there are several possible applications in many fields. The paper presents 4 examples :

- **Shapes Analysis of 3D Helices :** One motivation for studying shapes of cylindrical helices comes from protein structure analysis. Here, the objective is to deform one helical into another.

- **3D Face Recognition :** This is a very large problem that can be applied in homeland security, client access systems, video games etc. The challenge is to recognize people despite changes in shapes due to facial expressions, changes in the orientation of the face etc.
- **Elastic Models for Planar Shapes :** From a set of observed shapes, the goal is to develop a probability model to measure the variability of the observed data.
- **Transportation of Shape Deformations :** If we know how a known object deforms under a change of orientation, the idea is to assume that if we apply the same deformation to a new but similar object, then we can predict its deformation under the same change of orientation.

These examples are just a drop in the bucket, there are many more possible applications. As a result, to analyze shapes in $\mathbb{R}^n$, it is relevant to think about Square-Root Velocity representation and the elastic metric. This is notably the case in medical image analysis, computer vision, biology, etc.

3 MATHEMATICAL FRAMEWORK

In order to effectively analyze the shape of curves, a suitable mathematical representation is required, the aim being to construct a *shape space*. To do so, the authors first construct a *pre-shape space* containing the representation of the curves with appropriate constraints. Then, they regroup curves that are the same by shape-preserving transformations (rotations, translations, scaling, as well as re-parameterizations). This resulting quotient space is the desired *shape space*.

3.1 Square-Root Velocity representation

While there are a number of different approaches that have been proposed in the literature, the authors of this paper propose the use of the Square-Root Velocity representation (SRV) in order to construct a representation for the shapes.

Let $\beta : D \to \mathbb{R}^n$ be a parametrized curve. We define the continuous map $F : \mathbb{R}^n \to \mathbb{R}^n$ by $F(v) = \frac{v}{\sqrt{\|v\|}}$ if $\|v\| \neq 0$ and 0 otherwise, where $\|\cdot\|$ denotes the euclidean 2-norm in $\mathbb{R}^n$. From there, we represent the shape of β using the square-root velocity (SRV) function :

$$q : \begin{cases} D \to \mathbb{R}^n \\ t \mapsto F(\dot{\beta}(t)) = \frac{\dot{\beta}}{\sqrt{\|\dot{\beta}\|}} \end{cases}$$

FIGURES 1 and 2 show examples of a closed curve β_1 and an open curve β_2, with their corresponding SRV representations.

For every $q \in \mathbb{L}^2(D, \mathbb{R}^n)$ there exists a unique curve β (up to a translation), such that q is the SRV function of β. Indeed, for a given q, the associated curve is given by $\beta(t) = \int_0^t q(s)\|q(s)\| \, ds$. Therefore, we can work with q instead of β. This also removes the translations from the problem.

To remove scale variability, we can rescale all the curves to have unit length, resulting in $\int_D \|\dot{\beta}(t)\| \, dt = \int_D \|q(t)\|^2 \, dt = 1$. This implies that the SRV functions corresponding to rescaled curves are elements of the hypersphere in $\mathbb{L}^2(D, \mathbb{R}^n)$, denoted C^o. we can consider the domain D as the interval [0,1] for open curves.
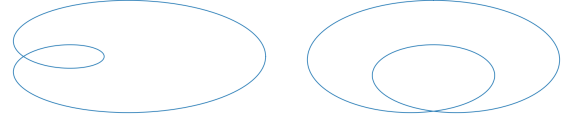

Figure 1: Closed curve β_1 (left) and its SRV representation (right). $\beta_1(t) = \begin{pmatrix} \cos(t)(0.5 + \cos(t)) \\ \sin(t)(0.5 + \cos(t)) \end{pmatrix}$
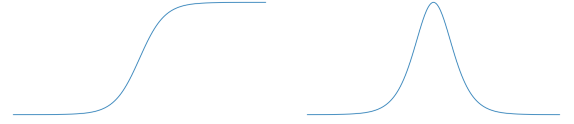

Figure 2: Open curve β_2 (left) and its SRV representation (right). $\beta_2(t) = \frac{1}{1+e^{-t}}$

For the case of closed curves, it is natural to consider the domain D as the unit circle $\mathbb{S}^1$. Then, the closure condition for these curves can be written as $\int_{\mathbb{S}^1} q(t)\|q(t)\| \, dt = 0$. It follows that we can define the space of fixed-length closed curves represented by their SRV functions as :

$$C^c = \left\{ q \in \mathbb{L}^2(D, \mathbb{R}^n) \mid \int_{\mathbb{S}^1} \|q(t)\|^2 \, dt = 1, \int_{\mathbb{S}^1} q(t)\|q(t)\| \, dt = 0 \right\}$$

3.2 Riemannian structure

Subsequently, we want to define Riemannian structures on those resulting pre-shape spaces C^o and C^c. To do so, we consider their tangent spaces.

For the open curves : Since C^0 is a sphere, its tangent space at a point q is given by

$$T_q(C^o) = \{v \in \mathbb{L}^2([0, 1], \mathbb{R}^n) \mid \langle v, q \rangle = 0\}$$

with $\langle v, q \rangle = \int_0^1 \langle v(t), q(t) \rangle dt$.

For the closed curves : The tangent space to C^c at a point q is

$$T_q(C^c) = \left\{ v \in \mathbb{L}^2(\mathbb{S}^1, \mathbb{R}^n) \mid \langle v, w \rangle = 0, \quad \forall w \in N_q(C^c) \right\}$$

where $N_q(C^c)$ is the normal space at q :

$$N_q(C^c) = \text{span} \left\{ q(t), \left(\frac{q_i(t)}{\|q(t)\|} q(t) + \|q(t)\| \mathbf{e}_i \right), i = 1, \dots, n \right\}$$

This normal space is defined using the directional derivatives of the function $q \mapsto \int_{\mathbb{S}^1} q(t)\|q(t)\| dt$.

The standard metric on $\mathbb{L}^2(D, \mathbb{R}^n)$ restricts to Riemannian structures on the two manifolds C^o and C^c. Then these structures can be utilized to determine geodesics and measure the length of the geodesics between elements of these spaces.

3.3 Geodesics

Let C be a Riemannian manifold, denoting either C^o or C^c, and $\alpha : [0, 1] \to C$ be a parameterized path such that $\alpha(0) = q_0$ and $\alpha(1) = q_1$. Then, the length of the path α is $L[\alpha] = \int_0^1 \sqrt{\langle \dot{\alpha}(t), \dot{\alpha}(t) \rangle} dt$.

We can then define the geodesic distance between q_0 and q_1 as

$$d_c(q_0, q_1) = \inf_{\substack{\alpha:[0,1]\to C \\ \alpha(0)=q_0, \alpha(1)=q_1}} L[\alpha]$$

3.4 Constructing the shape spaces

C^c and C^o are two pre-shapes spaces that we can turn into shape spaces by removing the re-parametrizations and the rotations, since we have already taken care of translations and scaling.

A rotation is an element of $\mathcal{SO}(n)$, and a re-parametrization is an element of Γ, the set of all orientation-preserving diffeomorphisms of D. Then, we can define group actions of $\mathcal{SO}(n)$ and Γ on the SRV of a curve.

The action of $\mathcal{SO}(n)$ is

$$\begin{aligned} \mathcal{SO}(n) \times C &\to C \\ (O, q) &\mapsto Oq \end{aligned}$$

For a $\gamma \in \Gamma$, the composition $\beta \circ \gamma$ denotes its re-parameterization. Then, the SRV of the re-parameterized curve is $F(\dot{\beta}(\gamma(t))\dot{\gamma}(t)) = q(\gamma(t))\sqrt{\dot{\gamma}(t)}$ with q the SRV of β. Consequently, we can define the action :

$$\begin{aligned} C \times \Gamma &\to C \\ (q, \gamma) &\mapsto (q \circ \gamma)\sqrt{\dot{\gamma}} \end{aligned}$$

Since these two actions commute, we can define a joint action of the product group $(\mathcal{SO}(n) \times \Gamma) \times C \to C : ((O, \gamma), q) \mapsto O(q \circ \gamma)\sqrt{\dot{\gamma}}$.

We can prove that this action is by isometries w.r.t the metric $\langle u, v \rangle = \int_D \langle u(t), v(t) \rangle dt$. Thanks to the isometric property, we can form the quotient space $C/(\Gamma \times \mathcal{SO}(n))$

The orbit of a function $q \in C$ is given by :

$$[q] = \{O(q \circ \gamma)\sqrt{\dot{\gamma}} \mid (\gamma, O) \in \Gamma \times \mathcal{SO}(n)\}$$

Then, we define the quotient space $\mathcal{S} = \{[q] \mid q \in C\}$. More precisely, we mod out by the closures of these orbits to use the property that if a compact Lie group H acts freely on a Riemannian manifold M by isometries, and if the orbits are closed then the quotient M/H is a manifold and inherits a Riemannian metric from M. Since $\Gamma \times \mathcal{SO}(n)$ acts by isometries, we mod out by the closures of the orbits (as they are not closed).

The geodesic distance between two points of $\mathcal{S}$ is :

$$d_s([q_0], [q_1]) = \inf_{(\gamma, O) \in \Gamma \times \mathcal{SO}(n)} d_c(q_0, O(q_1 \circ \gamma)\sqrt{\dot{\gamma}})$$

3.5 Motivation of the SRV Representation

In the preceding literature, the commonly used representation for a parametrized curve $\beta : D \to \mathbb{R}^n$ (s.t. for all $t, \dot{\beta}(t) \neq 0$), was the two functions :

$$\phi : \begin{cases} D \to \mathbb{R} \\ t \mapsto \ln\left(\|\dot{\beta}(t)\|\right) \end{cases}$$

$$\theta : \begin{cases} D \to \mathbb{S}^{n-1} \\ t \mapsto \dfrac{\dot{\beta}(t)}{\|\dot{\beta}(t)\|} \end{cases}$$

Intuitively, the function ϕ represents the log-speed of the curve, while the function θ indicates the direction of the curve. Together, ϕ and θ provide a complete description of the curve's shape and

motion. These two functions completely define β since $\dot{\beta}(t) = e^{\phi(t)}\theta(t)$. This defines a map from the space of open curves in $\mathbb{R}^n$ to $\Phi \times \Theta$ where Φ and Θ are sets of smooth maps.

Then, we impose a Riemannian structure with the tangent space of $\Phi \times \Theta$ at (ϕ, θ) given by

$$T_{(\phi,\theta)}(\Phi \times \Theta) = \Phi \times \{v \in \mathbb{L}^2(D, \mathbb{R}^n) \mid v(t) \perp \theta(t), \forall t \in D\}$$

Finally, we define the elastic metric on $\Phi \times \Theta$. For $(u_1, v_1), (u_2, v_2) \in T_{(\phi,\theta)}(\Phi \times \Theta)$, with a, b positive real numbers :

$$\begin{aligned} \langle (u_1, v_1), (u_2, v_2) \rangle_{(\phi,\theta)} = a^2 &\int_D u_1(t) u_2(t) e^{\phi(t)} \, dt \\ + b^2 &\int_D \langle v_1(t), v_2(t) \rangle e^{\phi(t)} \, dt \end{aligned}$$

The first integral is a measure of the stretching since u_1, u_2 are variations of the log-speed of the curve and the second integral is a measure of the bending since v_1, v_2 represent the variations of the direction of the curve. The coefficients a, b are leverages to penalize the stretching and/or the bending.

With this new representation, the action of $O \in \mathcal{SO}(n)$ is given by : $(O, (u, v)) = (u, Ov)$ where $(u, v) \in T_{(\phi,\theta)}(\Phi \times \Theta)$ and $(u, Ov) \in T_{(\phi, O\theta)}(\Phi \times \Theta)$. Indeed, rotations change the direction, not the speed. The action of $\beta \in \Gamma$ is given by $(\gamma, (u, v)) = (u \circ \gamma, v \circ \gamma)$ where $(u, v) \in T_{(\phi,\theta)}(\Phi \times \Theta)$ and $(u \circ \gamma, v \circ \gamma) \in T_{(\gamma,(\phi,\theta))}(\Phi \times \Theta)$

Since the shape of curves can be identified to $\Phi \times \Theta$, we can identify $(\Phi \times \Theta)/(\mathcal{SO}(n) \times \Gamma)$ to the space of shapes.

If we go back to the SRV representation, we can re-write it in terms of (ϕ, θ) as $q(t) = e^{\frac{1}{2}\phi(t)}\theta(t)$.

We can show that for $(u, v) \in T_{(\phi,\theta)}(\Phi \times \Theta)$, the corresponding tangent vectors to $\mathbb{L}^2(D, \mathbb{R}^n)$ at q given by $f = \frac{1}{2}e^{\frac{1}{2}\phi}u\theta + e^{\frac{1}{2}\phi}v$. Then, for f_1, f_2 two tangent vectors, we can compute the $\mathbb{L}^2$ inner product :

$$\begin{aligned} \langle f_1, f_2 \rangle &= \int_D \langle \frac{1}{2}e^{\frac{1}{2}\phi}u_1\theta + e^{\frac{1}{2}\phi}v_1, \frac{1}{2}e^{\frac{1}{2}\phi}u_2\theta + e^{\frac{1}{2}\phi}v_2 \rangle \, dt \\ &= \int_D \left(\frac{1}{4}e^{\phi}u_1u_2 + e^{\phi}\langle v_1, v_2 \rangle\right) \, dt \end{aligned}$$

So, with $a = \frac{1}{2}$ and $b = 1$ we have a correspondence between the $\mathbb{L}^2$ metric on the space of SRV representations and the elastic metric on $\Phi \times \Theta$. In other words, when we study a curve in $\mathbb{R}^n$, thanks to the SRV representation we can transport this study to a $\mathbb{L}^2$ space endowed with its metric, which is way easier to manipulate.

3.6 Computation of geodesics

3.6.1 For open curves.

Since C^o is a sphere, for $q_0, q_1 \in C^o$, a geodesic connecting them is given by

$$\alpha : \begin{cases} [0, 1] \to C^o \\ t \mapsto \dfrac{1}{\sin(\theta)}\left(\sin(\theta(1-t))q_0 + \sin(\theta t)q_1\right) \end{cases}$$
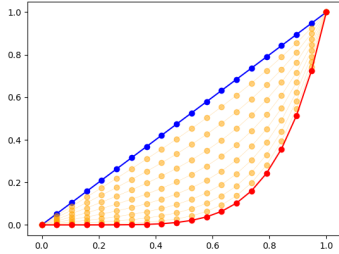
with $\theta = \cos^{-1}(\langle q_0, q_1 \rangle)$

To illustrate the computation of geodesics, we took an example with two open curves $\beta_0(t) = t$ and $\beta_1(t) = t^6$. The associated normalized SRV are $q_0(t) = 1$ and $q_1(t) = \sqrt{6}t^{2.5}$.

We compute and represent the geodesic in the SRV space, then we represent this geodesic in the original space of curves.
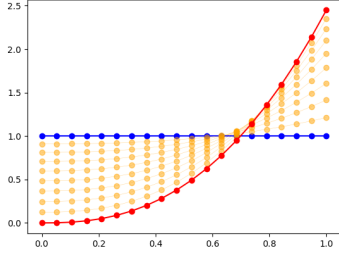
(a) Geodesic in the SRV space

(b) Geodesic in the original space

Figure 3: Geodesic in the SRV space (top) and geodesic in the curves space (bottom). The blue line represents β_0, the red one β_1 and the orange ones are sampled along the shortest path.

3.6.2 For closed curves.

Unfortunately, the geometry of C^c is not as simple. Therefore, for two closed curves $q_0, q_1 \in C^c$, the geodesic path cannot be computed the same way. The method presented in the article is a path-straightening method.

First, we start with an arbitrary path $\alpha : [0, 1] \rightarrow C^c$ such that $\alpha(0) = q_0$ and $\alpha(1) = q_1$. Then, we iteratively straighten α until we find a local minimum of the energy :

$$E(\alpha) = \frac{1}{2} \int_0^1 \langle \frac{d\alpha}{dt}(t), \frac{d\alpha}{dt}(t) \rangle \, dt$$

We state without proof, that a critical point of E is a geodesic on C^c.

To keep it simple, we get rid of technical details, to only present the main steps of the algorithm which finds a geodesic between two curves β_0 and $\beta_1 \in C^c$. We denote $\mathcal{H}$ the set of all paths in C^c and $\mathcal{H}_0$ the subset of $\mathcal{H}$ that starts at q_0 and end at q_1. The tangent space is denoted $\mathcal{T}_\alpha(\mathcal{H})$. $\mathcal{H}$ is endowed with the Palais metric $\langle\langle w_1, w_2 \rangle\rangle = \langle w_1(0), w_2(0) \rangle + \int_0^1 \langle \frac{Dw_1}{dt}(t), \frac{Dw_2}{dt}(t) \rangle dt$.

(1) Compute the SRV representations of $\beta_0, \beta_1 : q_0, q_1$.
(2) Initialize a path α between q_0 and q_1 in C^o and project it in C^c.
(3) Compute the velocity vector field $\frac{d\alpha}{dt}$ along the path α.

(4) Compute the covariant integral of $\frac{d\alpha}{dt}$ denoted u. A vector field $u \in T_\alpha(\mathcal{H})$ is called a covariant integral of $w \in T_\alpha(\mathcal{H})$ along α if $\frac{Du}{dt} = w$, with $\frac{Du}{dt}$ the covariant derivative of u along α, i.e. the vector field obtained by projecting $\frac{du}{dt}(t)$ onto $T_{\alpha(t)}(C^c)$ for all t.
(5) Compute the backward parallel translation of $u(1)$ along α denoted by $\tilde{v}$. u is the backward parallel translation of $w_1 \in T_{\alpha(1)}(C^c)$ along α if u is the forward parallel translation of w_1 along $\tilde{\alpha} : t \mapsto \alpha(1 - t)$. u is called the forward parallel translation of $w_0 \in T_{\alpha(0)}(C^c)$ along α if and only if $u(0) = w_0$ and $\frac{Du}{dt}(t) = 0$ for all t.
(6) Compute the full gradient vector field of the energy E along the path α denoted by w using w(t)=u(t)-t$\tilde{u}_1(t)$
(7) Update α along the vector field w. For $\varepsilon > 0$, if $\sum_{t=1}^k \langle w(t), w(t) \rangle < \varepsilon$, then stop, else return to step 3.

3.7 Comparison with other works

When $n = 1$, there is no angle component θ. Then, the elastic metric is $\langle u_1, u_2 \rangle_\phi = a^2 \int_D u_1(t)u_2(t)e^{\phi(t)} dt$. On the space of probability density functions $\mathcal{P} = \{p : [0, 1] \rightarrow \mathbb{R} | p \geq 0, \int_0^1 p(s)ds = 1\}$, we can recognize the Fisher-Rao metric for $a = 1 : \forall p \in P, \forall v_1, v_2 \in T_p(\mathcal{P}), \langle v_1, v_2 \rangle = \int_0^1 v_1(s)v_2(s)\frac{1}{p(s)}ds$. Under the square root representation, i.e. for $q(t) = e^{\frac{1}{2}\phi(t)}$, this metric reduces to the $\mathbb{L}^2$ metric defined in the section 3.5.

When $n = 2$, *A metric on shape space with explicit geodesics* by Younes [10] presents a framework to compute geodesics. They identify $\mathbb{R}^2$ with the complex plane $\mathbb{C}$ and define a Sobolev-type metric on plane curves that has the property of being isometric to some manifolds (Stiefel, Grassman, complex projective, sphere). With this framework, there is a closed-form formula to compute geodesics for open curves.

For $n > 2$, *Shape analysis of elastic curves for Euclidean spaces* [7] is the first work that discussed an SRV-type representation.

4 APPLICATIONS

To illustrate this framework in the context of shape analysis, we used the implementation of the SRV metric developed by Geomstats [5] on two examples.

4.1 Shape analysis of cancerous cell

This use case studies Osteosarcoma (bone cancer) cells and the impact of drug treatment on their morphological shapes, by analyzing cell images obtained from fluorescence microscopy. The dataset contains cells affected by two treatments (jasplakinolide and cytochalasin D), as well as a control sample.

We can study to which extent this metric can detect the association between the cell shape and its response to a treatment. Indeed, biological cells adopt a variety of shapes, determined by multiple processes and biophysical forces under the control of the cell. As metrics defined on the shape space of curves, the elastic metrics implemented in Geomstats are a potential tool for analyzing and comparing biological cell shapes. Their associated geodesics and geodesic distances provide a natural framework for optimally matching, deforming, and comparing cell shapes.

FIGURE 4 shows the geodesic between a control cell and another one under treatment. We clearly see that the shapes are really different. The metric we build can thus be used to automatically classify cells.

(a) A geodesic between two cells (from top left to bottom right).
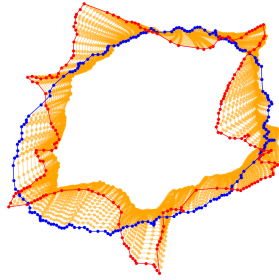
(b) Overlaid geodesic between the two cells

Figure 4: A geodesic between two cells

The Elastic metric on the space of curve also allows to calculate statistics on the dataset, such as the Karcher mean :

$$\mu = \arg\min_{[q]\in\mathcal{S}^c} \sum_{i=1}^{n} d_s\left([q],[q_i]\right)^2$$

FIGURE 5 shows how far each treatment is from the Karcher mean. We notice that the cells under treatment are further away from the mean, especially for the cytochalasin D treatment. This confirms that the treatments do have an impact on cell shape.
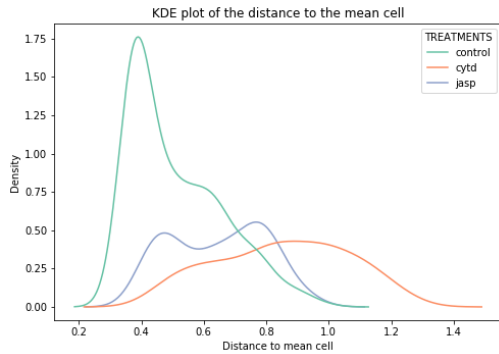
Figure 5: KDE plot of the distance from the cancerous cells and the Karcher mean of the dataset.

4.2   Leaf analysis

Another possible application is the analysis of leafs. Indeed, leaves have really specific forms. It can be useful in the field of agriculture to automatically monitor plants. Some plant diseases can lead to abnormal shapes, for example.

In this use case, we use the Swedish Leaf dataset, which is a dataset generated by a leaf classification project at Linköping University and the Swedish Museum of Natural History [6], which contains 15 species of leaves, with 75 images per species for a total of 1125 images. To use shape analysis, we first extract the contours of the leaves with OpenCV.
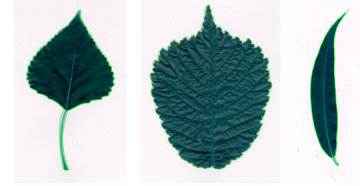

Figure 6: Examples of leaves from the dataset and the contouring done with OpenCV

From these curves, we can look at the means of each class, to have an idea of the usual shape for the leaves. We restrained ourselves to a small subset for readability reasons, we selected 5 leaves for 3 classes.

FIGURE 7 shows the Karcher mean for each class. The resulting curve represents the leaves really well. Therefore, the distance between a new leave, not in the subset and the means of each class, can be used to classify the leaves. TABLE 1 shows the distance between new leaves and the previous Karcher means. Indeed, we see that each leaf is closer to its class' mean.
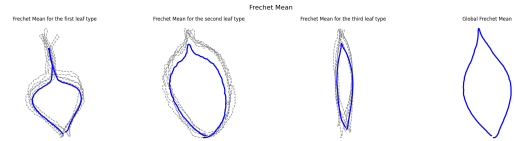

Figure 7: Karcher mean (blue) on a subset of the dataset divided by type of plant and the global Karcher mean. The subset is plotted

To go a bit further, it is easy to cluster the leaves with the Elastic metric and a hierarchical clustering. FIGURE 8 shows such a clustering. The Elastic metrics manages to separate each class nicely.

5   LIMITS AND DISCUSSION

5.1   Generalization to surfaces

The general framework is about curves $\beta : D \rightarrow \mathbb{R}^n$ with $D = [0,1]$ or $\mathbb{S}^1$ but we can wonder about the generalization of this method to surfaces. We can consider maps $f : D \rightarrow \mathbb{R}^3$ where D is a two-dimensional compact spaces, for example :

- $D = [0,1]^2$: f is called a quadrilateral surface

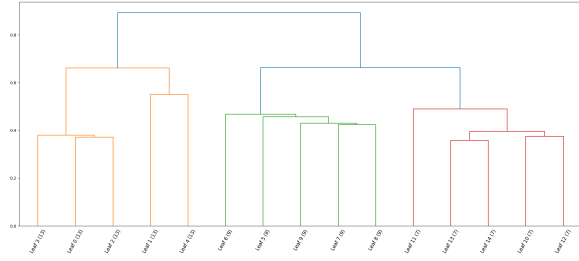**Table 1: Distance between new test leaves and the previously calculated Karcher mean of each class.**

Figure 8: Dendrogram of the hierarchical clustering on the subset of leaves using complete linkage.

- $D = \mathbb{S}^2$: f is called a spherical surface
- $D = \mathbb{S}^1 \times [0, 1]$: f is called a disc surface

Then, there exists many possible representations for f :

- **Gradient Field :** $\nabla f : \mathbb{S}^2 \to \mathbb{R}^{3 \times 2}$.
  ∇f is invariant to translation of f but not to rotation, scale and re-parametrization. We can reconstruct f from ∇f.
- **Normal Vector Fields :** For $s = (u, v) \in \mathbb{S}^2$, the normal vector field is $\tilde{n}(s) = \frac{\partial f}{\partial u} \times \frac{\partial f}{\partial v}$. The unit normal vector field is $n(s) = \frac{\tilde{n}(s)}{\|\tilde{n}(s)\|}$.
  The map $n : s \in \mathbb{S}^2 \mapsto n(s) \in \mathbb{S}^2$ is called the Gauss map of f, and the set of all Gauss maps is $C^\infty(\mathbb{S}^2, \mathbb{S}^2)$.
  $n(s)$ is invariant to translation of f but not rotation and re-parametrization. We can't reconstruct f from n.
- **Tensor Field :** $g(s) = \nabla f(s)^T \nabla f(s)$.
  The space of all g's is the set of all Riemannian metrics on $\mathbb{S}^2$, denoted Met($\mathbb{S}^2$).
  $g(s)$ is invariant to translation and rotation of f but not re-parametrization. We can't reconstruct f from g.
- Finally, we can define the area element $r(s) = \|\tilde{n}(s)\| = \sqrt{\det(g(s))}$

We can represent a surface f as the pair (g, n). Then, the group actions are :

- **Translation :** $f \mapsto f + x$, $(g, n) \mapsto (g, n)$

- **Rotations :** $f \mapsto Of$, $(g, n) \mapsto (g, On)$
- **Scaling :** $f \mapsto af$, $(g, n) \mapsto (a^2 g, n)$
- **Re-parametrization :** $f \mapsto f \circ \gamma$, $(g, n) \mapsto (J_\gamma^T (g \circ \gamma) J_\gamma, n \circ \gamma)$

Let $(\delta g_1, \delta n_1), (\delta g_2, \delta n_2)$ represent two tangent vectors of the representation space at the point (g, n).

We can adapt the elastic Riemannian metric previously defined to this new problem :

$$
\begin{aligned}
\langle\langle (\delta g_1, \delta n_1), (\delta g_2, \delta n_2) \rangle\rangle_{(g,n)} &= a \int_{\mathbb{S}^2} \text{Tr}((g^{-1}\delta g_1)_0 (g^{-1}\delta g_2)_0) r(s) \mathrm{d}s \\
&= b \int_{\mathbb{S}^2} \text{Tr}(g^{-1}\delta g_1) \text{Tr}(g^{-1}\delta g_2) r(s) \mathrm{d}s \\
&= c \int_{\mathbb{S}^2} \langle \delta n_1, \delta n_2 \rangle r(s) \mathrm{d}s
\end{aligned}
$$

where a, b, c are positive weights and $A_0 = A - Tr(A)$.

This metric can be interpreted as the sum of a shape term, a stretching term and a bending term.

Then, we can define the equivalent of the square root velocity, called the Square Root Normal Field : $q = \sqrt{r}n$

5.2 Hypothesis of the absolute continuity of β

If we try to use the SRV for functions that aren't absolutely continuous, various things can go wrong. For example, if the function isn't differentiable almost everywhere, its SRV won't be defined since it uses the derivative. If you allow functions that are differentiable almost everywhere but not absolutely continuous, then two different functions might have the same SRVF. For example, the Cantor function has derivative = 0 almost everywhere, so it would be the same as a constant function using the SRVF. The smoothness is also important because ultimately we would like to find diffeomorphic mappings between the SRV functions. In practice, we can numerically smooth the curves β.

5.3 Discontinuous shapes

The paper doesn't deal with discontinuous shapes or shapes that make abrupt discontinuous jumps in parametrization. These will result in non-diffeomorphic solutions when doing shape matching. This issue is related to the one we discussed in the previous section.

5.4 Unicity of the geodesic

In section 3.6, we stated that a critical point of E is a geodesic on C^c. But, there can exist multiple geodesics between two points q_0, q_1, then, a local minimum of E is not always a minimizing geodesic. We are not ensured that the minimizing geodesic is reached with the presented algorithm, but we only reach a geodesic between the two points.

5.5 Generalization to function $\beta : \mathbb{R} \to M$

This is a difficult question and there are several approaches to apply the SRVF method to curves in more general Riemannian manifolds. We can cite *Computing distances and geodesics between manifold-valued curves in the SRV framework* by Alice Le Brigant [1]. The author uses the SRVF to define a Riemannian metric on the space of immersions $Imm([0, 1], M)$ with M a Riemannian manifold. This induces a first-order Sobolev metric on this space. As in our paper,

there exists a correspondence between the $\mathbb{L}^2$ metric in the SRV representation spaces and the Sobolev metric on $Imm([0,1], M)$.

5.6 Locality of the gradient

An important limitation of the gradient method is that its solution is always local. If we want to apply this method, it should converge to a local minimum, but if we initialize using a different starting point, it might converge to a different local minimum. A solution could be to use dynamic programming that gives a global solution to an approximate problem. This problem is not specific to our paper, but we think that it's relevant to keep this in mind while we work with gradient method.

Another issue due to the locality of solutions arises when we compute mean shapes. For example, the definition of Karcher mean is a local minimum. Thus we may get different solutions depending on the initial conditions. To overcome this limitation, we can think of approaches such as barycenters or seeding the initial condition (mean) randomly from the population multiple times and then choose the best solution (that minimizes the sum squared error).

5.7 Example of the non-application of the elastic metric

Shape spaces built based on elastic metrics are invaluable to study populations of biological objects following a priori unknown distributions. Unfortunately, due to the non-linear geometry of these shape spaces, most of the traditional data analysis techniques can only be applied after a linearization step (projection onto a tangent space). An alternative way to explore distributions of biological shapes is to exploit representation learning and build a linear latent shape space in an unsupervised manner. However, this type of learned representation does not explicitly encode invariance as a true shape space should.

The recently-proposed Kendall Shape-VAE[8] combined the best of these two worlds by learning a latent space with a simple geometry that is invariant to similitude transformations. Parameterization invariance, the key feature of elastic shape spaces, is however not included. Some researchers at EMBL-EBI study how parameterization invariance can be incorporated in a learning framework based on VAEs and try to propose an Elastic Shape-VAE that builds up on the Kendall Shape-VAE.

6 CONCLUSION

In conclusion, shape analysis has applications in many fields. Building a rigorous set of theoretical and computational tools is therefore mandatory. In the paper from Srivastava et al. [7], the focus is on building a shape space for boundary models, especially elastic curves in Euclidean spaces, instead of using landmarks which are often subjective. They introduce a new representation for curves, the Square-Root Velocity representation, that allows to find geodesics between open and closed curves in $\mathbb{R}^n$. This framework is pretty useful since it allows to work in the $\mathbb{L}^2$ space endowed with its metric instead of working in the space of curves with a more complicated metric. This paper has been an important contribution in the study of shape spaces and led to the publications of many papers on the subjects.

We illustrated this method on two examples, to look at the effects of treatments on cancerous cell and to study the shapes of leaves. The results were satisfying since we succeed to highlight the utility of the treatment in the first example, and to classify the leaves in the second example.

However, this method applies to absolutely continuous curves in $\mathbb{R}^n$, so it doesn't deal with surfaces, manifold-valued functions or discontinuous shapes. Some articles published after this one discuss this problem and present some solutions . Moreover, we don't have any theoretical guarantees about the unicity of the geodesic or about the convergence to a global minimum.

REFERENCES

[1] Alice Le Brigant. 2016. Computing distances and geodesics between manifold-valued curves in the SRV framework. *arXiv preprint arXiv:1601.02358* (2016).

[2] David G Kendall. 1977. The diffusion of shape. *Advances in applied probability* 9, 3 (1977), 428–430.

[3] David G Kendall and Wilfrid S Kendall. 1980. Alignments in two-dimensional random sets of points. *Advances in Applied probability* 12, 2 (1980), 380–424.

[4] Washington Mio, Anuj Srivastava, and Shantanu H. Joshi. 2007. On Shape of Plane Elastic Curves. *International Journal of Computer Vision* 73 (2007), 307–324.

[5] Nina Miolane, Nicolas Guigui, Alice Le Brigant, Johan Mathe, Benjamin Hou, Yann Thanwerdas, Stefan Heyder, Olivier Peltre, Niklas Koep, Hadi Zaatiti, Hatem Hajri, Yann Cabanes, Thomas Gerald, Paul Chauchat, Christian Shewmake, Daniel Brooks, Bernhard Kainz, Claire Donnat, Susan Holmes, and Xavier Pennec. 2020. Geomstats: A Python Package for Riemannian Geometry in Machine Learning. *Journal of Machine Learning Research* 21, 223 (2020), 1–9. http://jmlr.org/papers/v21/19-027.html

[6] Oskar Söderkvist. 2001. Computer vision classification of leaves from swedish trees.

[7] Anuj Srivastava, Eric Klassen, Shantanu H Joshi, and Ian H Jermyn. 2010. Shape analysis of elastic curves in Euclidean spaces. *IEEE transactions on pattern analysis and machine intelligence* 33, 7 (2010), 1415–1428.

[8] Sharvaree Vadgama, Jakub Mikolaj Tomczak, and Erik J Bekkers. 2022. Kendall Shape-VAE: Learning Shapes in a Generative Framework. In *NeurIPS 2022 Workshop on Symmetry and Geometry in Neural Representations*.

[9] Laurent Younes. 1998. Computable elastic distances between shapes. *SIAM J. Appl. Math.* 58, 2 (1998), 565–586.

[10] Laurent Younes, Peter W Michor, Jayant M Shah, and David B Mumford. 2008. A metric on shape space with explicit geodesics. *Rendiconti Lincei* 19, 1 (2008), 25–57.